Available online at www.sciencedirect.com
ScienceDirect
Journal of Power Sources 179 (2008) 81–86
JOURNAL OF POWER SOURCES
www.elsevier.com/locate/jpowsour

Short communication

A polyoxometalate-deposited Pt/CNT electrocatalyst via chemical synthesis for methanol electrooxidation

Min Ho Seo, Sung Mook Choi, Hyung Ju Kim, Jae Hong Kim, Beong Ki Cho, Won Bae Kim *

Department of Materials Science and Engineering, Gwangju Institute of Science and Technology (GIST), Cheomdan-gwagiro, Gwangju 500-712, South Korea

Received 1 September 2007; received in revised form 22 October 2007; accepted 11 December 2007
Available online 11 January 2008

Abstract

Polyoxometalate anion $PMo_{12}O_{40}^{3-}$ (POM) is chemically impregnated into a Pt-supported carbon nanotubes (Pt/CNTs) catalyst that is prepared via a colloidal method. The POM-impregnated Pt/CNTs catalyst system (Pt/CNTs-POM) shows at least 50% higher catalytic mass activity with improved stability for the electrooxidation of methanol than Pt/CNTs or POM-impregnated Pt/C (Pt/C-POM) catalyst systems. The enhancement in electrochemical performance of the Pt/CNTs-POM catalyst system can be attributed to the combined beneficial effects of improved electrical conductivity due to the CNTs support, highly dispersed Pt nanoparticles on the CNTs, and increased oxidation power of the polyoxometalate that can assist oxidative removal of reaction intermediates adsorbed on the Pt catalyst surface.

Keywords: Polyoxometalate; Platinum catalyst; Carbon nanotubes; Direct methanol fuel cell; Enhanced activity; Methanol oxidation

1. Introduction

The direct methanol fuel cell (DMFC), which is generally fabricated with an acidic polymer electrolyte and Pt-based electrodes, has been increasingly attracting attention as a clean alternative power source for portable electronic devices. It offers the advantages of high-specific energy density and good conversion efficiency of methanol fuel at a relatively low operating temperature [1,2]. Prior to further implementation, however, technological problems such as low power density due to sluggish oxidation reactions at the Pt-based anode, fuel crossover from negative (anode) to positive (cathode) electrode, and the high price and limited supply of the electrode catalysts have yet to be overcome [1]. To improve electrocatalyst systems in DMFC electrodes with economical use of the Pt content, alternative supports, various bimetallic catalysts and modified preparation methods have been developed. For instance, carbon nanotubes (CNTs) have drawn increasing attention in recent years for their applications as electrocatalyst supports [3–7] because the CNTs have good electrical properties, chemical stability in acidic electrolyte conditions and high specific surface-area.

Polyoxometalates (POMs) are inorganic clusters with oxometalates that can be readily prepared through the coordination chemistry of a central heteroatom surrounded by addenda ions of metal oxides [8]. Due to their electrochemical redox properties and oxidizing abilities, the POMs have been applied to various kinds of acid-catalyzed oxidation reactions [9,10]. Also it was demonstrated that Keggin-type $PMo_{12}O_{40}^{3-}$ anions in an aqueous solution could effectively assist the electrochemical oxidation of carbon monoxide (CO) with water molecules to carbon dioxide (CO_2) over gold catalysts [11,12], as represented by

$$CO(g) + H_2O(l) + PMo_{12}O_{40}^{3-}(aq) \rightarrow CO_2(g) + 2H^+(aq) + PMo_{12}O_{40}^{5-}(aq) \quad (1)$$

Note that CO is a byproduct that is generally produced during the electrooxidation of methanol, but it should be catalytically or electrochemically removed from the fuel electrode as CO can seriously poison Pt-based electrocatalysts [5]. As the POM anion has been shown to be readily adsorbed on gold, carbon and mer-

* Corresponding author. Tel.: +82 62 970 2317; fax: +82 62 970 2304.
E-mail address: wbkim@gist.ac.kr (W.B. Kim).

0378-7753/$ – see front matter © 2008 Elsevier B.V. All rights reserved.
doi:10.1016/j.jpowsour.2007.12.107

cury electrodes [13–15], as well as, on the surface of CNTs [16], there was a report to demonstrate that $PMo_{12}O_{40}^{3-}$ anions were incorporated into CNT supports and that POM-modified CNT composites could be employed as a good support for methanol electrooxidation, in which Pt or PtRu was electrochemically deposited on POM-modified CNTs that were mounted on a pyrolytic graphite (PG) electrode [16].

A colloidal method for nanoparticle formation has been widely employed to prepare Pt-based fuel cell catalysts with narrow particle size distribution and high dispersion [17–19]. Thus, POM modification of Pt/CNT catalysts made from this colloidal preparation would provide a further advantage for DMFC electrode catalysts by utilizing the oxidizing power of the POM. POMs are easily decomposed, however, by hydrolysis in aqueous basic solutions [20] that is normally employed in the colloidal synthesis process with reducing agents of polyols [17].

We report here that POM-impregnated Pt/CNT (hereafter denoted as Pt/CNT-POM) can be obtained by simple chemical synthesis methods, in which highly dispersed Pt nanoparticles are first prepared and deposited on to the surface of CNTs via a polyol-based colloid method, and POMs can be subsequently deposited on to the Pt/CNTs in an aqueous solution. Their catalytic properties in terms of mass activity and stability for methanol electrooxidation are then compared with Pt/CNTs, Pt/C-POM or PtRu/C to investigate the effects of CNTs and POM over the chemically prepared Pt/CNT-POM catalyst systems.

2. Experiment

The CNTs (Iljin Nanotech Co., CM-95, BET surface area = 200 $m^2\ g^{-1}$) were ultrasonicated and stirred in an acid solution of HNO_3 and HCl with a volume ratio of 1:3 for 12 h to purify and activate the CNT supports. The CNTs were then filtered and washed with distilled water (18.2 MΩ cm) [21] and dried by vacuum freeze-drying to prevent aggregation. Next, the CNT-supported Pt catalysts (20 wt.% in metal loading) were prepared through a colloidal method with ethylene glycol, in which the latter served as a reductant for Pt^{2+} ions and a stabilizer for the Pt colloidal nanoparticles [22]. In a typical procedure, the activated CNTs were ultrasonicated for 4 h in ethylene glycol solution to avoid CNT agglomeration, and then an ethylene glycol solution containing $H_2PtCl_6{\cdot}6H_2O$ (Aldrich Chem. Co.) was mixed with the CNT-dispersed solution using magnetic stirring. As the next step, a NaOH solution was added dropwise until the pH of the solution reached around 12, before the solution was refluxed at an elevated temperature of 433 K for 3 h. After the temperature cooled to 298 K, colloidal Pt nanoparticles were produced in the solution bath. This solution was stirred for 24 h to ensure all Pt nanoparticles were deposited on to the CNTs, at which point the solution became transparent. The Pt/CNT catalyst mixture was then filtered and washed several times with pure ethanol and distilled water, and dried by vacuum freeze-drying for 48 h.

POM modification on the prepared Pt/CNT catalysts was carried out as follows: 0.4 g of 20 wt.% Pt/CNTs was suspended in 50 ml of 5.48×10^{-5} mol $H_3PMo_{12}O_{40}$ (Aldrich) solution in a 2:1 volume ratio of distilled water (18.2 MΩ cm) and 2-propanol solution, i.e., a 4:1 weight ratio of the catalyst and $H_3PMo_{12}O_{40}$. The mixture was ultrasonically scattered for 30 min to prepare a well-dispersed and homogeneous catalyst ink, and further mixed with a vortex mixer for 12 h to allow the POMs to adsorb on to the catalyst. Finally, the Pt/CNT-POM catalysts were filtered and washed with distilled water several times and dried in an oven at 373 K for 2 h in a nitrogen atmosphere.

X-ray diffraction (XRD) analyses of the catalysts were carried out with a Rigaku Rotalflex (RU-200B) X-ray diffractometer using a Cu Kα (λ = 1.5405 Å) source with a nickel filter to characterize the crystalline Pt structures of all Pt-based catalysts. The source was operated at 40 kV and 100 mA, and the 2θ angular region between 15° and 85° was explored at a scan rate of 3° min^{-1}. The morphology and size distribution of the Pt/CNT catalysts with and without POMs were then investigated by means of transmission electron microscopy (TEM, JEOL JEM-2100) operated at 200 kV. All TEM samples were prepared by ultrasonically suspending the catalyst particles in an ethanol solution. Drops of these suspensions were deposited on to a standard copper grid (200 mesh) covered with a carbon film and dried for 20 min to allow the ethanol and water to evaporate. To measure and compare the activity based on the Pt mass, an inductively coupled plasma mass spectrophotometer (ICP-MS, VG Elemental Ltd.) was employed for composition measurements.

A glassy-carbon working electrode (WE) was consecutively polished in 1, 0.3 and 0.05 μm Al_2O_3 pastes (ALLIED High Tech Products Inc.) until the WE surface became mirror-like. The WE was electrochemically activated and cleaned in a 0.5-M sulfuric acid solution with a linear sweep of potential at 100 mV s^{-1}, from 0.1 to 1.5 V for 30 cycles. Catalyst inks were then prepared as follows: Pt/C (E-Tek), Pt/CNTs (homemade), Pt/CNTs-POM (homemade) and PtRu/C (E-Tek) catalysts were suspended with sonication for 0.5 h in a solution mixture of distilled water, 2-propanol and 5 wt.% Nafion solution (Aldrich). The ratio of catalyst and Nafion polymer was 74 wt.%:26 wt.%. Next, 3 μl of the catalyst ink was transferred with a micropipette to the activated, clean surface of the glassy-carbon disc electrode (with geometric area of *ca.* 0.07 cm^2 and a Pt loading of 5.48 ± 0.05 μg), followed by drying in an oven at 343 K for 0.5 h, to form eventually a thin film of the catalyst layer. The electrooxidation performance of the catalysts were investigated using cyclic voltammetry (Solartron analytical 1400, AMETEK) with a three-electrode cell at room temperature. Glassy carbon (3-mm diameter) held in a Teflon cylinder was used as the working electrode, on which a thin layer of Nafion-impregnated catalyst was cast. An Ag/AgCl electrode and a Pt wire electrode were used as the reference and counter electrode, respectively. A solution of 2 M CH_3OH in 0.5 M H_2SO_4 was employed as the electrolyte solution and electrochemical measurements were performed after degassing with nitrogen of ultra-high purity. Cyclic voltammograms (CVs) were subsequently recorded within the potential range of −0.2 to 1.0 V (vs. Ag/AgCl) at a scan rate of 50 mV s^{-1}; long-term stability tests of each sample were performed for up to 500 cycles and compared under the same conditions.

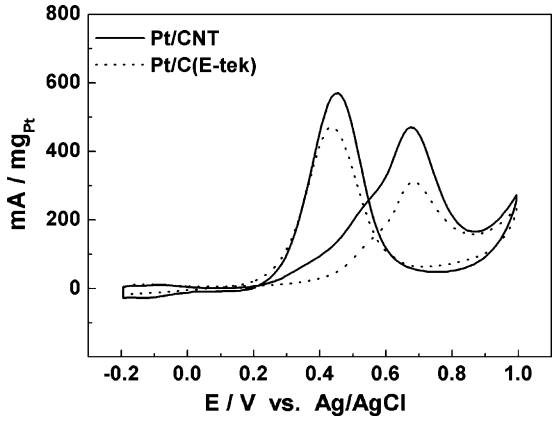

Fig. 1. Cyclic voltammograms for tenth cycle of Pt/CNT (solid line) and Pt/C (dotted line) in electrolyte solution of 0.5 M H_2SO_4 with 2 M CH_3OH at a sweep rate of 50 mV s^{-1} at room temperature. Same Pt loadings mounted in all cases.

3. Results and discussion

Fig. 1 shows the cyclic voltammograms (CVs) of the synthesized Pt/CNT and commercial Pt/C catalysts in an electrolyte solution of 0.5 M H_2SO_4 + 2 M CH_3OH. There are two irreversible current peaks during the electrooxidation of methanol that are typically attributed on the forward scan peak at around 0.7 V to methanol electrooxidation and on the backward peak at *ca.* 0.4 V, to the Faradaic oxidation reaction on the Pt of residual intermediate species such as CH_2OH, CH_2O, HCOOH and CO [23,24]. Both CV curves reveal a similar shape and peak position, which is also in agreement with previous reports for methanol CVs over supported Pt catalysts [5,23]. However, the oxidation current peak observed for the Pt/CNT catalysts (solid line in Fig. 1) appears to be considerably higher (by *ca.* 50%) than the peak for the commercially available Pt/C catalyst (dotted line) when compared per same Pt mass. This improvement in the electrocatalytic performance of the Pt/CNTs compared with that of carbon black-supported Pt could be attributed to the presence of CNT supports with unique structural and electrical properties that can reduce resistances associated with charge transfer [3–5].

Another factor enabling high mass activity would be the high dispersion of metal catalysts on the supports [21] through the production of uniformly nanosized Pt particles, in which the functionalized CNT surface allows uniform adsorption of the Pt nanoparticles produced via a polyol method. The unique structural and electrical properties of CNTs are believed to be a dominant factor for the higher activity in this work, since the mean diameter of Pt on the CNT supports appears to be not significantly different from that of C-supported Pt (*ca.* 3.1 nm as estimated from TEM images of the Pt/C catalyst). Although the electrochemical active surface area (EAS) of the catalysts without POM modification, measured in aqueous 0.5 M sulfuric acid solution without methanol from the hydrogen desorption region, is estimated to be *ca.* 73.8 and 109.6 $m^2\ g^{-1}$ for Pt/C and Pt/CNT in this work, respectively, such a difference in EAS values over the similar mean particle size of Pt on both supports should be therefore attributed to the unique structural and electrical properties of the CNT supports.

The morphology of the CNT supports and the prepared Pt/CNT catalysts, shown in Fig. 2 reveals that the Pt nanoparticles are highly dispersed on the CNT supports, with a mean particle size of *ca.* 2.9 ± 0.1 nm. The size distribution and mean size of the Pt nanoparticles were estimated from the average measurements of more than 300 particles seen in the TEM image. The high dispersion of the Pt nanoparticles on the CNT supports could be achieved through two mechanisms: (i) surface functional groups such as carboxyl, hydroxyl and carbonyl groups on the CNTs could be effectively produced during chemical oxidation treatment [21], and they should assist ion adsorption and metal deposition by serving as specific nucleation sites for Pt nanoparticles; (ii) the polyol employed during Pt/CNT synthesis enables Pt nanoparticle uniformity on CNT surfaces, acting as both a reductant for Pt cations and a protective agent by stabilizing the nanosized particle surface from particle growth [25–28].

In order to enhance the oxidation ability of Pt/CNT catalysts for methanol electrooxidation, POM anions were adsorbed over the prepared Pt/CNT catalysts through spontaneous and strong chemisorption of POMs on to the surface of CNTs [14] in an aqueous solution. The presence and adsorption of the POMs on

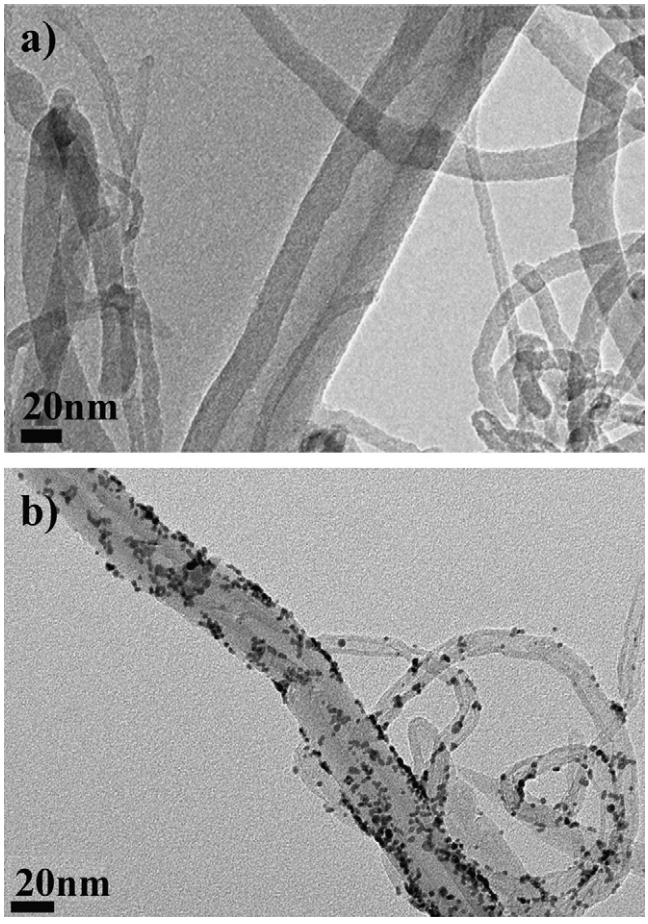

Fig. 2. Transmission electron microscopy images of (a) CNTs and (b) 20 wt.% Pt/CNTs used in this work.

both the CNT and Pt/CNT materials are evident by the characteristic redox peaks in the CVs of Fig. 3, which were measured at a scanning rate of 50 mV s^{-1} in acidic electrolyte solutions of 0.5 M H_2SO_4 and 0.5 M H_2SO_4 + 2 M CH_3OH, respectively, at room temperature. In Fig. 3(a), whereas the CV for CNTs alone is represented by a typical electrical double-layer feature [7] without any charge transfer reactions, the POM-adsorbed CNTs reveal multiple and reversible redox peaks originating from the electrochemical redox reactions of POMs with electrons on the CNTs [16,29]. The CV waves during the first cycle for the Pt/CNTs-POM (see arrows in Fig. 3(b)) also show typical multiple redox peaks of the POMs on the catalyst surface in acidic electrolyte solution containing 0.5 M H_2SO_4 + 2 M CH_3OH, suggesting that the POMs are unequivocally adsorbed again on to the surface of the Pt/CNT catalysts. Note that there are no such peaks in the case of Pt/CNTs without POM adsorption.

Fig. 4 shows the electrochemical activity pertaining to methanol oxidation in the Pt/C, Pt/C-POM, and Pt/CNT-POM catalyst systems; the voltammograms of the Pt/CNT-POM and Pt/C-POM electrodes have considerably greater oxidation currents by at least 50% than those without the POM, and the Pt/CNT-POM catalysts show a superior performance over the other systems. Considering that the same amount of Pt is used in this work, the activity enhancements are achieved by *ca.* 50%

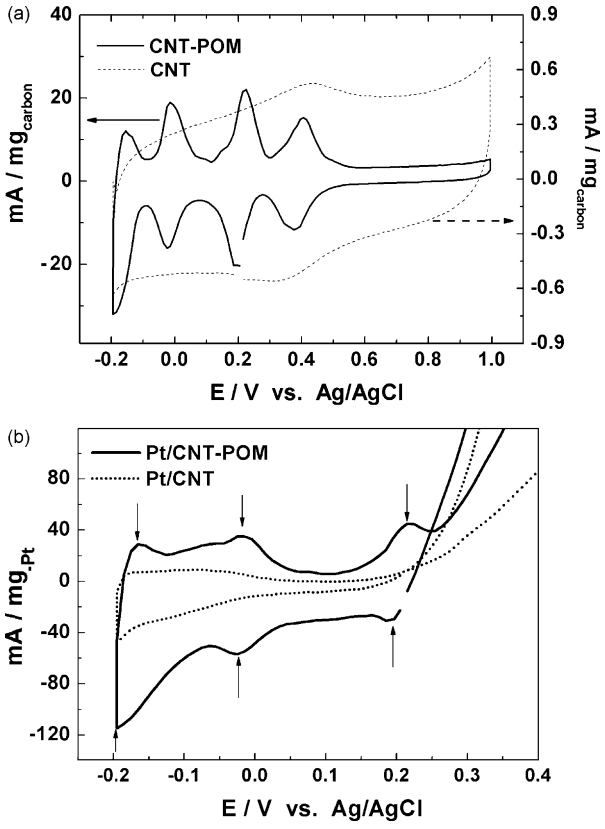

Fig. 3. (a) Cyclic voltammograms of CNTs with or without POM in 0.5 M H_2SO_4 electrolyte at a scan rate of 50 mV s^{-1} at room temperature. (b) CVs for first cycle for Pt/CNTs-POM (solid line) and Pt/CNTs (dotted line) over enlarged potential range of −0.2 to 0.4 V (vs. Ag/AgCl) in 0.5 M H_2SO_4 containing 2 M CH_3OH solution at 50 mV s^{-1} at room temperature.

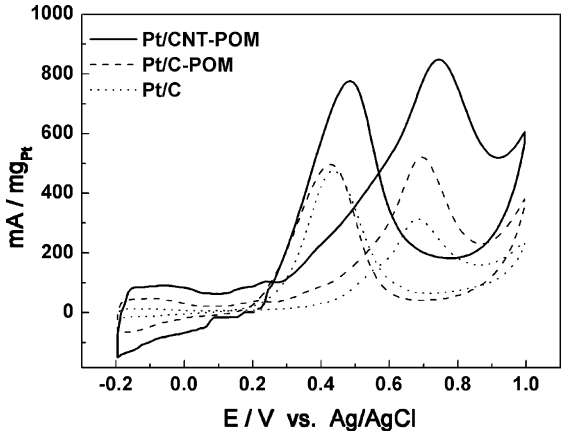

Fig. 4. Cyclic voltammograms for tenth cycle for Pt/CNTs-POM (solid line), Pt/C-POM (dashed line), and Pt/C (dotted line) in 0.5 M H_2SO_4 containing 2 M CH_3OH solution at 50 mV s^{-1} at room temperature. Same Pt loadings mounted in all cases.

improvement with CNT supports instead of carbon black supports, as shown in Fig. 1. Further improvement by at least 50% is obtained with POM introduction to the catalyst system, as presented in Fig. 4. These results can be understood as follows: (i) the presence of CNTs provides an efficient support for the Pt nanoparticles along with economical use and enhanced electrical conductivity of the electrode process compared with the carbon black [19]; (ii) the presence of POM anions may facilitate the electrooxidation of intermediate species such as the CO that is adsorbed on the Pt catalyst surfaces, as demonstrated elsewhere [11,12], leading to suppression of the poisoning effect on Pt catalysts by CO or CO-like intermediates. From different points of view, it can be inferred from the increase in the hydrogen desorption peaks in the potential range of −0.2 to 0.1 V that the active Pt surface is less-poisoned by CO or CO-like intermediates in cases of POM modification due to their oxidation reaction capabilities.

The oxidative removal of intermediate species can be deduced from the peak current intensity ratio between the forward peak current I_f and the backward peak current I_b, in which the latter is generally recognized as the current produced during the electrooxidation of residual intermediate species on the Pt surface after methanol electrooxidation [5,30,31]. Note that the ratio I_f/I_b is less than 1 in Fig. 1 for the cases of Pt/CNT and Pt/C without POM, but the ratios became greater than unity for the cases with POM, as seen in Fig. 4. Therefore, the current peak ratio I_f/I_b can be used to indicate catalyst tolerance against the formation of poisoning species on the Pt catalyst surfaces [5,30,31]. Whereas the oxidation current peak appearing during the forward potential scan corresponds to the electrochemical oxidation reactions of methanol, the current peak occurring during the backward potential scan is attributed to the oxidation reactions of intermediate species produced from the incomplete oxidation of methanol during the forward scan. Thus, the anodic peak current in the backward scan detected at around 0.4 V in this study is primarily associated with the removal of the incompletely oxidized carbonaceous species produced and adsorbed on the Pt surface. For example, with CO as one of the poisoning

species to the Pt formed during methanol oxidation, the electrochemical oxidation reaction of CO taking place during the backward potential scan is [5]:

$$\text{Pt–OH} + \text{Pt} = \text{C} = \text{O} \rightarrow \text{CO}_2 + 2\text{Pt} + \text{H}^+ + \text{e}^- \quad (2)$$

Without POM modification on the catalysts, the I_f/I_b ratios are 0.66 for the Pt/C and 0.82 for the Pt/CNT, but increase in the presence of POMs to 1.04 and 1.09 for the Pt/C-POM and Pt/CNT-POM catalysts, respectively. These increases correspond to a relative reduction of the backward peak current, implying that less CO species remain to be adsorbed on the Pt surface (i.e., poisoned state) after methanol electrooxidation. Therefore, POM-deposited catalyst systems can be viewed as being more tolerant to poisoning species such as CO on Pt.

Although the presence of POM anions on Pt/CNT catalysts is confirmed by their characteristic redox waves in the CV tests, it would be interesting to investigate the state of the POM anions on the catalysts. First, the amount of POMs on the Pt/CNTs catalyst was determined by ICP-MS analysis, which showed that *ca.* 9.6 wt.% of $PMo_{12}O_{40}^{3-}$ anions are deposited on the Pt/CNTs, in which approximately 50% of the POMs added initially remained in a strongly adsorbed state on the Pt/CNT catalysts, and others are removed during preparation steps such as washing and filtering. Also, the relative Pt loading is estimated to be *ca.* 17.4 wt.% compared with the CNT supports. In addition, XRD analysis was used to examine the Pt/CNT, CNT-POM and Pt/CNT-POM systems in terms of the structural phase of Pt and POM if the latter forms a crystalline phase, as shown in Fig. 5. The XRD pattern of the Pt/CNT catalysts represents the characteristic peaks of a crystalline face-centered-cubic (fcc) Pt phase as it shows the planes (1 1 1), (2 0 0), and (2 2 0) at the corresponding diffraction positions. In the CNT-POM electrode, the diffraction peaks at around 20°, 25°, and 43° are associated with the (1 1 0), (0 0 2), and (1 0 0) planes of the hexagonal structure of CNT supports [22], with no noticeable diffraction peaks in the measurements that may be contributed by crystallized POMs or Mo oxides. Furthermore, no other diffraction patterns are observed in the Pt/CNTs-POM catalyst system except for

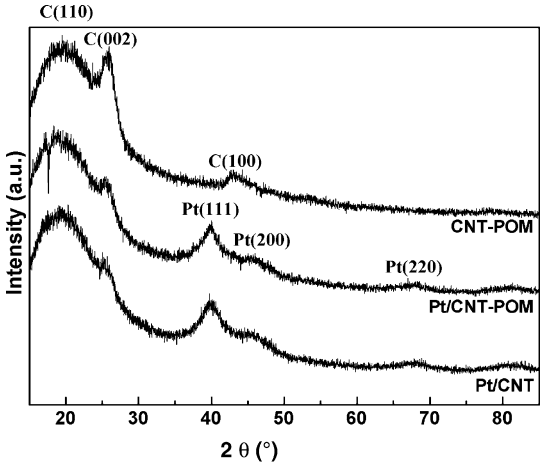

Fig. 5. X-ray diffraction patterns of CNTs-POM, Pt/CNTs-POM and Pt/CNTs over scan range 10–85°.

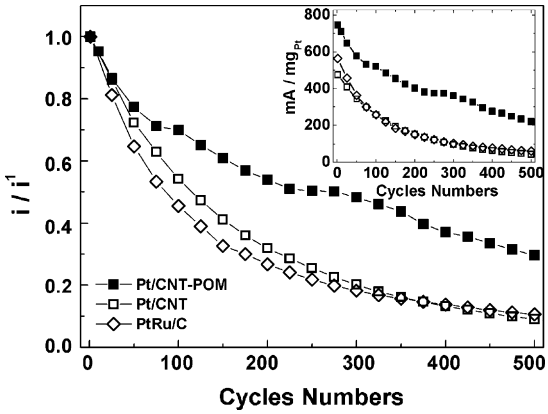

Fig. 6. Long-term cycle stability of Pt/CNTs-POM, Pt/CNTs and PtRu/C electrodes in 0.5 M H_2SO_4 containing 2 M CH_3OH solution at 50 mV s^{-1} at room temperature. Same Pt loadings mounted in all cases.

similar fcc-Pt diffraction peaks as the Pt/CNT catalysts. Thus, it can be concluded from the XRD analysis that the POMs are adsorbed in a highly dispersed manner on the Pt/CNT catalysts with no agglomeration, and the crystallographic structure of the Pt nanoparticles is not affected by the presence of POMs.

Pt-based electrocatalysts have been reported to degrade during long-term stability tests of low-temperature fuel cells [32,33] or from cyclic voltammetry performances in an acid [32], methanol [16] and ethanol [34] containing electrolyte solutions. In our chemically prepared Pt/CNT-POM catalyst system, the stability issues involved in the Pt and support would exist analogously; thus, the stability of POMs should also be considered. For this reason, the long-term stability tests shown in Fig. 6 were performed, in which current profiles are plotted as a ratio of the forward peak current (i) measured at the corresponding CV cycle divided by the current (i^1) at the first cycle taken after full activation of the catalyst systems; the actual current intensity profiles are also included for reference in the inset figure. For comparison, the long-term cycle stability of the commercially available PtRu/C electrode is also shown and compared with our catalyst systems. It is found that both the PtRu/C and Pt/CNT electrodes have almost the same performance in that similar current profiles result with cycle number. Also, the ratio of i/i^1 appears to be decreased at slightly faster rates with cycles as compared with that of the Pt/CNT-POM catalyst system. After the 500th cycle on the PtRu/C or the Pt/CNTs catalyst, approximately 90% of the electrocatalytic initial activity has been lost, showing an i/i^1 ratio of about 0.1, while the Pt/CNT-POM electrocatalyst experiences a smaller activity loss of 70% from the initial activity (note that the i/i^1 ratio is still greater than 0.3 at the 500th cycle). It is more interesting to consider the actual current profile (see the inset in Fig. 6), in which the specific current is substantially greater (>250 mA mg_{Pt}^{-1}) even at the 500th cycle for the Pt/CNT-POM, whereas the catalyst systems without POMs showed less than 50 mA mg_{Pt}^{-1}. Consequently, the Pt/CNT-POM system showed superior performance for the electrochemical oxidation of methanol, including greater activity and better stability over repeated tests. Thus the Pt/CNT-POM catalysts prepared from the chemical synthetic method in this work have economical potential in terms of efficient Pt usage as

an anode in DMFCs. Nevertheless, further studies are required to understand the adsorption state of POM anions on the Pt/CNT catalyst surface and the mechanistic scheme for POM roles in enhancing the activity of the Pt/CNT catalysts for methanol electro oxidation.

4. Conclusions

The polyoxometalate anion $PMo_{12}O_{40}{}^{3-}$ (POM) was chemically impregnated into Pt-supported carbon nanotube (Pt/CNT) catalysts. The Pt/CNT-POM catalysts have superior Pt-based mass activities with improved stability in the electrooxidation of methanol, as compared with Pt/CNTs, Pt/C, and PtRu/C. The enhancements in activity and stability over Pt/CNT-POM catalyst systems have been attributed to several combined beneficial effects, such as: (i) improved electrical conductivity of the CNTs; (ii) highly dispersed Pt nanoparticles on the CNTs via a polyol process; (iii) enhanced oxidation power of methanol due to the presence of POMs for facilitating the oxidative removal of poisoning species on Pt. These findings suggest that Pt/CNT-POMs should be considered a good electrocatalyst material for DMFCs or other direct alcohol fuel cells, with potential for use in the reduction of Pt use and the replacement of another precious metal such as Ru in fuel cell anode materials.

Acknowledgements

This work was supported by New & Renewable Energy R&D Program (2005-N-FC03-P-01-0-000) under the Korea Ministry of Commerce, Industry and Energy (MOCIE) and the Korea Research Foundation Grant of the Korean Government (MOEHRD) (KRF-2005-205-D00023).

References

[1] M. Winter, R.J. Brodd, Chem. Rev. 104 (2004) 4245.
[2] G.A. Olah, Angew. Chem. Int. Ed. 44 (2005) 2636.
[3] T.W. Ebbensen, H.J. Lezec, H. Hiura, J.W. Bennett, H.F. Ghaemi, T. Thio, Nature 382 (1996) 54.
[4] R.H. Baughman, A.A. Zakjidov, W.A.d. Heer, Science 297 (2002) 787.
[5] Y. Mu, H. Liang, J. Hu, L. Jiang, L. Wan, J. Phys. Chem. B 109 (2005) 22212.
[6] N.M. Rodriguez, M.S. Kim, R.T.K. Baker, J. Phys. Chem. 98 (1994) 13108.
[7] G. Che, B.B. Lakshmi, E.R. Fisher, C.R. Martin, Nature 393 (1998) 346.
[8] C.L. Hill, C.M. Prosser-McCartha, Coord. Chem. Rev. 143 (1995) 407.
[9] N. Mizuno, M. Misono, Chem. Rev. 98 (1998) 199.
[10] M. Zhoua, L.P. Guo, F.Y. Lin, H.X. Liu, Anal. Chim. Acta 587 (2007) 124.
[11] W.B. Kim, T. Voitl, G.J. Rodriguez-Rivera, J.A. Dumesic, Science 305 (2004) 1280.
[12] W.B. Kim, T. Voitl, G.J. Rodriquez-Rivera, S.T. Evans, J.A. Dumesic, Angew. Chem. Int. Ed. 44 (2005) 778.
[13] C. Rong, F.C. Anson, Anal. Chem. 66 (1994) 3124.
[14] D.E. Katsoulis, Chem. Rev. 98 (1998) 359.
[15] M. Sadakane, E. Steckhan, Chem. Rev. 98 (1998) 219.
[16] D. Pan, J. Chen, W. Tao, L. Nie, S. Yao, Langmuir 22 (2006) 5872.
[17] N. Toshima, Y. Wang, Langmuir 10 (1994) 4574.
[18] Y. Wang, J. Ren, K. Deng, L. Gui, Y. Tang, Chem. Mater. 12 (2000) 1622.
[19] T. Matsumoto, T. Komatsu, K. Arai, T. Yamazaki, M. Kijima, H. Shimizu, Y. Takasawa, J. Nakamura, Chem. Commun. 7 (2004) 840.
[20] A. Jürgensen, J.B. Moffat, Catal. Lett. 34 (1995) 237.
[21] W. Li, C. Liang, W. Zhou, J. Qiu, Z. Zhou, G. Sun, Q. Xin, J. Phys. Chem. B 107 (2003) 6292.
[22] Y. Xing, J. Phys. Chem. B 108 (2004) 19255.
[23] S. Park, Y. Xie, M.J. Weaver, Langmuir 18 (2002) 5792.
[24] V.S. Bagotzky, Y.B. Vassiliev, O.A. Khazova, J. Electroanal. Chem. 81 (1977) 229.
[25] F. Fievet, J.P. Lagier, B. Blin, B. Beaudoin, M. Figlarz, Solid State Ionics 32/33 (1989) 198.
[26] G. Viau, F. Fiévet-Vincent, F. Fiévet, Solid State Ionics 84 (1996) 259.
[27] P.Y. Silvert, R.H. Urbina, N. Duvauchelle, V. Vijayakrishnan, K.T. Elhsissen, J. Mater. Chem. 6 (1996) 573.
[28] P.Y. Silvert, R. Herrera-Urbina, K. Tekaia-Elhsissen, J. Mater. Chem. 7 (1997) 293.
[29] A. Kuhn, F.C. Anson, Langmuir 12 (1996) 5481.
[30] Y. Zhu, H. Uchida, T. Yajima, M. Watanabe, Langmuir 17 (2001) 146.
[31] Z. Chen, L. Xu, W. Li, M. Waje, Y. Yan, Nanotechnology 17 (2006) 5254.
[32] J. Zhang, K. Sasaki, E. Sutter, R.R. Adzic, Science 315 (2007) 220.
[33] P. Yu, M. Pemberton, P. Plasse, J. Power Sources 144 (2005) 11.
[34] M.Y. Wang, J.H. Chen, Z. Fan, H. Tang, G.H. Deng, D.L. He, Y.F. Kuang, Carbon 42 (2004) 3251.